J. Fluid Mech. (1965), *vol.* 21, *part* 3, *pp.* 513–534
Printed in Great Britain

Vorticity amplification in stagnation-point flow and its effect on heat transfer

By S. P. SUTERA
Division of Engineering, Brown University, Providence, Rhode Island

(Received 31 January 1964)

Recently a mathematical model was proposed (Sutera, Maeder & Kestin 1963) to demonstrate that vorticity amplification by stretching was an important mechanism underlying the sensitivity of stagnation-point heat transfer on cylinders to free-stream turbulence. According to the model, vorticity of a scale larger than a certain neutral scale and appropriately oriented can undergo amplification as it is convected towards the boundary layer. Such vorticity, present in the oncoming flow with small intensity, can reach the boundary layer with a greatly magnified intensity and induce substantial three-dimensional effects therein. The mean temperature profile was shown to be much more responsive to these effects than the mean velocity profile and very large increases in the wall-heat-transfer rate were calculated for Prandtl numbers 0·74 and 7·0.

In this work a second, more general, case is treated in which the approaching flow carries vorticity of scale 1·5 times the neutral. By means of iterative procedures applied on an electronic analogue computer, an approximate solution to the full Navier–Stokes equation is generated. The heat-transfer problem is solved simultaneously for Pr = 0·70, 7·0 and 100. It is found that a vorticity input which increases the wall-shear rate by less than 3 % is capable of increasing the wall-heat-transfer rate by as much as 40 %. The sensitivity of the thermal boundary layer depends on Prandtl number. In the three cases investigated it is greatest for Pr = 7·0 and least for Pr = 100.

1. Introduction

The strong sensitivity of stagnation-point heat transfer on cylinders to the presence of turbulence in the free stream is well known and has been clearly demonstrated by experiments. Most theoretical investigations into the reasons for this sensitivity have considered the time dependence of the free-stream fluctuations as the essential feature to introduce into the boundary-layer analysis. The resulting analyses of laminar boundary layers with time-dependent, two-dimensional external flows have, however, failed to predict changes in the mean heat-transfer rates of anything like the large magnitudes measured in the laboratory (see, for example, Kestin, Maeder & Wang 1961).

In a recent paper Sutera *et al.* (1963) proposed that vorticity amplification due to stretching of vortex filaments in the diverging stagnation-point flow might be the essential underlying mechanism. A mathematical model was formulated,

and calculations based on it did reveal a significant difference in the respective sensitivities of the momentum and energy boundary layers to the presence of distributed vorticity in the flow approaching the stagnation point. A certain amount of distributed vorticity in the oncoming flow, capable of increasing the mean shear rate at the wall by only 5 %, caused the mean heat-transfer rate to rise by 26 % in a fluid with Prandtl number 0·74.

This theory also predicted that the scale of the vorticity being convected into the stagnation-point flow is an important factor in determining whether the vorticity will be amplified or not. A certain neutral scale was discovered for which amplification by stretching would be exactly balanced by viscous dissipation with the result that neutral-scale vorticity would approach the boundary layer with unvarying intensity. Vorticity of larger scale would experience net amplification while smaller-scale vorticity would be attenuated. The calculation described in the paper dealt, in fact, with the special case of the neutral scale. The history of this subject is extensively, although not exhaustively, discussed in the paper by Sutera *et al.* and need not be repeated here. There was, however, one note by Kuethe, Willmarth & Crocker (1959) which escaped mention in that discussion and which is particularly relevant since it contains experimental results in apparent accord with the main predictions of the vorticity-amplification theory. In the note, there are reported hot-wire measurements of velocity fluctuations near the noses of blunt bodies of revolution. The authors found that over a wide range of subsonic speeds the r.m.s. values of the fluctuations were considerably higher than those in the free stream and that most of the turbulent energy was in the frequency range 0–5 c/s. With the hot wire placed between 5 and 10 boundary-layer thicknesses from the surface, amplification ratios as high as 3 were measured for the u'/U_∞ fluctuation. It was further concluded that the preferential amplification of the low-frequency components in the free-stream fluctuations, usually attributed to vorticity fluctuations, indicated a mechanism causing amplification of vorticity fluctuations in the flow near the stagnation point. The stretching of vortex filaments was named as a possible cause.

Another question raised by the aforementioned results of Sutera *et al.* concerned the influence of Prandtl number on the sensitivity of the thermal boundary layer. Preliminary computations revealed that the effected increase in heat-transfer rate was substantially greater in a fluid with Prandtl number 7·0 than it was when $\mathrm{Pr} = 0{\cdot}74$. This finding was somewhat perplexing because it was expected that in the higher Prandtl-number fluid, in which the thermal boundary layer is thinner, the sensitivity to disturbances coming from without would be less.

It is the objective of the present paper to report the results of calculations pertaining to another more general application of the vorticity-amplification theory. In the following, a stagnation-point flow will be considered which, far from the boundary, contains distributed, unidirectional vorticity of a scale 1·5 times the neutral. It will be shown how this vorticity, given the appropriate orientation, is amplified as it approaches the boundary layer and induces signicant three-dimensional effects within the boundary layer. As a consequence the mean heat transfer may be substantially augmented. It is further shown that

with increasing Prandtl number the effect on heat transfer eventually diminishes but not monotonously. The effect is indeed larger in the case Pr = 7·0 than in the case Pr = 0·70 but smaller in the case Pr = 100 than in the latter.

2. Mathematical model

For a detailed development of the mathematical model the reader is referred to the original paper. In this section the physical process underlying the model will be re-emphasized, and only aspects of the mathematical development which are essential to the coherence of this paper will be given.

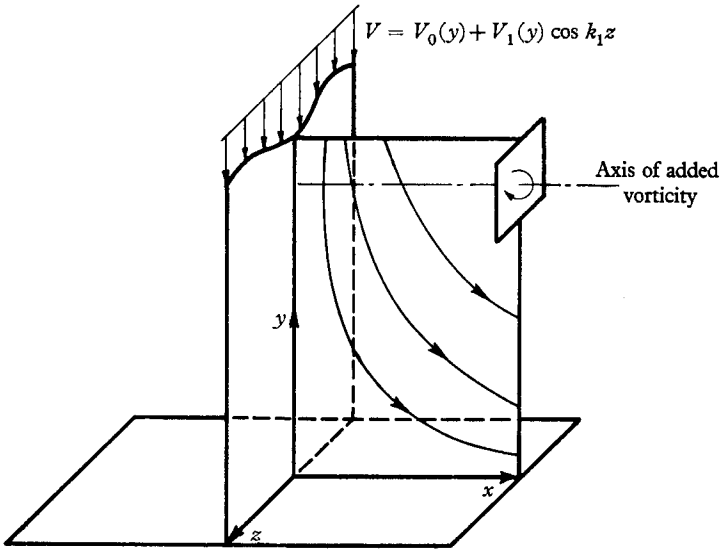

FIGURE 1. Sketch showing mode of vorticity addition.

Figure 1 shows the physical situation to be represented by the mathematical model: the steady flow of a viscous, incompressible fluid having constant properties into a plane stagnation-point. The problem is identical to that considered and first solved by Hiemenz (1911) except for the addition of distributed vorticity to the flow far from the boundary. The way in which this vorticity is added is portrayed in the figure. A simple sinusoidal variation is superimposed on the normal or y-component of velocity such that the associated vortex lines are parallel to the x-axis. This is the only one of the three components of a generally oriented vorticity which is susceptible to stretching in the stagnation-point flow. Under the simplifying restrictions of complete time independence, incompressibility, constant fluid properties and negligible viscous dissipation, the equations of vorticity and energy transport are then solved to determine the effect of the added vorticity on conditions near the boundary.

For convenience the problem is phrased in terms of dimensionless variables. Let the dimensional dependent variables be denoted by an asterisk superscript. Then the dimensionless variables are defined as follows:

(a) the co-ordinates

$$\xi, \eta, \zeta \equiv (a/\nu)^{\frac{1}{2}} x, \quad (a/\nu)^{\frac{1}{2}} y, \quad (a/\nu)^{\frac{1}{2}} z;$$

(*b*) the velocity vector

$$\mathbf{c} \equiv (a\nu)^{-\frac{1}{2}}\mathbf{c}^*;$$

(*c*) the rotation vector ($= \frac{1}{2}(\nabla \times \mathbf{c})$)

$$\boldsymbol{\omega} = \boldsymbol{\omega}^*/a;$$

(*d*) the temperature function

$$T = (T_w - T^*)/(T_w - T_\infty).$$

In these definitions the subscripts w and ∞ denote conditions at the wall and very far from the wall ($\eta \to \infty$), respectively, ν is the kinematic viscosity, and a is a constant of the stagnation flow having the dimension of reciprocal time. The constant a occurs naturally in the two-dimensional stagnation point flow through the conditions on the tangential and normal velocity components (x and y or ξ and η components) at the edge of the boundary layer, viz.

$$u^* \to ax, \quad v^* \to -ay + \text{const.}$$

as $\eta \to \infty$. In terms of the unbounded flow of an inviscid, incompressible fluid past a circular cylinder of diameter D, $a = 4V_\infty/D$, where V_∞ is the velocity of the uniform stream infinitely far from the cylinder.

The differential equations taken as governing the velocity and temperature boundary layers are the time-independent vorticity-transport equation, the incompressible continuity equation and the time-independent energy-transport equation with no dissipation. In terms of the dimensionless variables listed above these are

$$(\mathbf{c}.\nabla)\,\boldsymbol{\omega} = (\boldsymbol{\omega}.\nabla)\,\mathbf{c} + \nabla^2\boldsymbol{\omega}, \tag{1a}$$

$$\boldsymbol{\omega} = \tfrac{1}{2}(\nabla \times \mathbf{c}), \tag{1b}$$

$$\nabla.\mathbf{c} = 0, \tag{2}$$

$$(\mathbf{c}.\nabla)\,T = (1/\mathrm{Pr})\,\nabla^2 T. \tag{3}$$

They are subject to the boundary conditions:

$$\mathbf{c}(\xi, 0, \zeta) = 0, \tag{4}$$

$$T(\xi, 0, \zeta) = 0, \tag{5}$$

$$u \to \xi, \quad \partial v/\partial\eta \to -1, \quad w \to 0 \tag{6a,b,c}$$

and

$$T \to 1 \quad \text{as} \quad \eta \to \infty. \tag{7}$$

2.1. *Similarity hypothesis*

Solutions are sought which have the same underlying similarity as the Hiemenz flow but which are three dimensional. Thus the following similar forms are introduced:

$$\left.\begin{aligned} u &= U(\eta, \zeta)\,\xi, \\ v &= V(\eta, \zeta), \\ w &= W(\eta, \zeta), \\ T &= T(\eta, \zeta). \end{aligned}\right\} \tag{8}$$

The three components of vorticity in such a field are

$$2\boldsymbol{\omega}.\mathbf{i} = W_\eta - V_\zeta \equiv 2\Omega(\eta, \zeta), \tag{9}$$

$$2\boldsymbol{\omega}.\mathbf{j} = U_\zeta \xi, \tag{10}$$

$$2\boldsymbol{\omega}.\mathbf{k} = -U_\eta \xi. \tag{11}$$

where **i**, **j** and **k** are the usual unit vectors parallel to the ξ, η and ζ axes, respectively, and the subscripts denote differentiations.

It should be noted that the **k** component of vorticity is present in the classical Hiemenz problem. The other two components, however, are peculiar to this three-dimensional problem and of these only the **i** component is susceptible to stretching. Consequently attention will be focused on this one in what is to follow.

2.2. *Specification of Fourier structure*

As mentioned earlier, the addition of vorticity is to be accomplished by superimposing a simple sinusoidal variation on the normal or η velocity component far from the boundary. This is to say that as $\eta \to \infty$

$$V(\eta, \zeta) \to V_0(\eta) + V_1(\eta) \cos k\zeta. \tag{12}$$

Since the possibility of amplification of initially small deviations from the classical Hiemenz flow is of interest here, it will eventually be stipulated that V_1/V_0 be small at large values of η. According to the Hiemenz solution, V_0 is a function which increases linearly with η as $\eta \to \infty$; thus the stipulation will be obeyed by functions $V_1(\eta)$ which are bounded as $\eta \to \infty$. This particular point is important to the discussion which ensues and it will be expanded considerably later on.

The asymptotic behaviour specified above for the function V coupled with the condition that there be no net flow in the z (or ζ) direction leads rather naturally to the following assumed forms for the functions U, V, W and T:

$$U = U_0(\eta) + A \sum_{n=1}^{\infty} u_n(\eta) \cos k_n \zeta, \tag{13}$$

$$V = V_0(\eta) + A \sum_{n=1}^{\infty} v_n(\eta) \cos k_n \zeta, \tag{14}$$

$$W = A \sum_{n=1}^{\infty} k_n^{-1} w_n(\eta) \cos k_n \zeta, \tag{15}$$

$$T = T_0(\eta) + A \sum_{n=1}^{\infty} \theta_n(\eta) \cos k_n \zeta. \tag{16}$$

It follows from these and the definition (9) that

$$\Omega = A \sum_{n=1}^{\infty} \omega_n(\eta) \sin k_n \zeta, \tag{17a}$$

where

$$2\omega_n = [k_n^{-1} w_n' + k_n v_n]. \tag{17b}$$

(Here and hereafter the prime notation will always signify differentiation with respect to the variable η.)

The factor A will be called the amplitude parameter. It may be regarded as a normalizing device which allows the various summations to be considered as functions of order unity, but it also injects a certain flexibility into the problem

which is of great use when solving by analogue computer. Once the solutions are presented, however, it will be possible to assign a more physical meaning to A.

The k_n are dimensionless wave-numbers associated with the harmonic components of the periodically distributed vorticity. They are positive numbers, not necessarily integers, but $k_n = nk_1$ for all $n > 1$. With each wave-number there is associated a wavelength $\lambda_n = 2\pi/k_n$. The longest, or fundamental, wavelength is that associated with the first harmonic component, viz. $\lambda_1 = 2\pi/k_1$, and, as will be explained below, is a specified quantity. In analogy with a true turbulent flow the various wavelengths may be thought of as measures of eddy sizes and λ_1, therefore, as a measure of the largest eddy present.

Although the vorticity to be added to the flow far from the boundary will consist of a single harmonic component, of specified scale, it should be clear that the infinite spectra provided in equations (13) to (17) are necessary because the governing differential equations are basically non-linear. Excitation of a non-linear system by a single harmonic form will generally result in a distorted response containing both sub- and ultra-harmonic components. For this reason it should be expected that the equation governing any one of the components u_n, v_n, etc., will be coupled to all other components.

The statement that the largest eddy has a finite scale or, what is equivalent, that the smallest wave-number k_1 is not zero implies that generation of sub-harmonics does not occur. The fact is that in its present form the mathematical model does not provide for this possibility. Consequently, if a simple harmonic distribution of vorticity is imposed on the approaching stagnation flow the non-linear mechanisms which then act on this vorticity can generate only ultra-harmonic components. For this reason the wave-number specified for the added vorticity will necessarily be the smallest, viz. k_1. This feature of the model may at first appear unrealistic; but, if one recalls that observations of true turbulence indicate that, with few exceptions, energy transfer through the turbulent spectrum progresses from large scale to small scale, or that large eddies always break up into smaller ones and not vice versa, then there is a basis for it.

2.3. *Resulting system of ordinary differential equations*

Substitution of the velocity components as expressed by the equations (8), (13), (14) and (15) into the continuity equation (2) gives

$$U_0 + V_0' = 0, \tag{18}$$

and

$$u_n + v_n' + w_n = 0. \tag{19}$$

The first of these indicates that it is possible to introduce a single function to represent both U_0 and V_0. Thus let

$$\phi(\eta) \equiv -V_0, \tag{20}$$

whence

$$U_0 = \phi'. \tag{21}$$

Substitution of these same expressions plus (16) into the differential equations (1a) and (3) and the definition (1b) then leads, after some manipulation,

to the following set of ordinary differential equations governing the functions ϕ, T, u_n, v_n, ω_n and θ_n:

$$\phi''' + \phi\phi'' + \phi'^2 + 1 = A^2 \sum_{i=1}^{\infty} \{u_i^2 + \tfrac{1}{2}(u_i v_i)'\}, \tag{22}$$

$$T_0'' + \Pr \phi T_0' = \tfrac{1}{2} A^2 \Pr \sum_{i=1}^{\infty} \{u_i \theta_i + (v_i \theta_i)'\}, \tag{23}$$

$$u_n'' + \phi u_n' - (2\phi' + k_n^2) u_n - \phi'' v_n = \tfrac{1}{2} A \sum_{i=1}^{\infty} \{2u_i(u_{i+n} + u_{i-n} + u_{n-i}) + [v_i(u_{i+n} + u_{i-n} + u_{n-i})]' - (n/i) w_i(u_{i+n} - u_{i-n} - u_{n-i})\}, \tag{24}$$

$$-v_n'' + k_n^2 v_n = 2k_n \omega_n + u_n', \tag{25}$$

$$\omega_n'' + (\phi\omega_n)' - k_n^2 \omega_n = \tfrac{1}{2} A \sum_{i=1}^{\infty} \{[\omega_i(v_{n+i} + v_{n-i} - v_{i-n})]' - (n/i) w_i(\omega_{n+i} + \omega_{i-n} - \omega_{n-i})\}, \tag{26}$$

$$\theta_n'' + \Pr \phi \theta_n' - k_n^2 \theta_n - \Pr T_0' v_n = \tfrac{1}{2} A \Pr \sum_{i=1}^{\infty} \{[v_i(\theta_{n+i} + \theta_{i-n} + \theta_{n-i})]' + u_i(\theta_{n+i} + \theta_{i-n} + \theta_{n-i}) - (n/i) w_i(\theta_{n+i} - \theta_{i-n} - \theta_{n-i})\}. \tag{27}$$

In the summations i is a dummy index and quantities having subscripts such as $n-i$ or $i-n$ are to be replaced by zero whenever their subscripts are zero or negative.

Note that equations (22) and (23) are single equations whereas each of the equations (19) and (24) to (27) represents an infinite set since $1 \leqslant n < \infty$. Thus there are two plus a quintuple infinity of differential equations for the same number of unknowns so that the problem is determinate. The equations are all ordinary and, except for (22), linear. They are also coupled and, in principle, must be solved simultaneously.

2.4. *Boundary conditions*

The problem is essentially a two-point boundary-value problem and the boundary conditions are expressed by equations (4) to (7). Substitution of the assumed forms into (4) and (5) yields

$$\left.\begin{aligned} &\phi = \phi' = 0, \\ &T_0 = 0, \\ \text{and} \quad &u_n = v_n = w_n = \theta_n = 0 \quad \text{at} \quad \eta = 0. \end{aligned}\right\} \tag{28}$$

An additional condition due to the continuity relation (19) is

$$v_n'(0) = 0. \tag{29}$$

The boundary conditions (6) and (7) then require that

$$\left.\begin{aligned} &\phi' \to 1, \quad u_n \to 0, \quad v_n' \to 0, \quad w_n \to 0 \\ \text{and} \quad &T_0 \to 1, \quad \theta_n \to 0 \quad \text{as} \quad \eta \to \infty. \end{aligned}\right\} \tag{30}$$

Furthermore, this last set of conditions is taken to imply that all derivatives of these functions higher than those occurring in (30) vanish as $\eta \to \infty$.

3. The role of vorticity scale in the amplification process

The role of vorticity scale and the related concept of a neutral scale were discussed in the original paper by Sutera *et al.* That discussion leaned heavily on the matter of the asymptotic solution to equation (26) but was not entirely complete in this regard. Since this is a fundamental point in the theory it is definitely worthy of further attention and in this section an attempt will be made to redevelop the subject in a more thorough manner.

Equation (26) governs the behaviour of the individual harmonic components of that particular vector component of the vorticity (actually one-half the vorticity) which is susceptible to stretching. The right member of this equation represents the generating effect of interactions among the various harmonic components. It was stated in § 2.2 that a simple sinusoidal variation, characterized therefore by a unique wave-number k_1, would be superimposed on the flow field far from the boundary. As the vorticity associated with this 'ripple' is convected towards the boundary ($\eta = 0$) its intensity will change and eventually higher harmonics will be generated and the sinusoidal wave-form will distort. Beyond some sufficiently large value of η, however, this generation of higher harmonics will be so small that the effect of spectral interactions on the evolution of the initial wave-form can be neglected. When this is true, the corresponding ω_1 is effectively governed by the following asymptotic version of equation (26)

$$\omega_1'' + \phi\omega_1' + (\phi' - k_1^2)\,\omega_1 = 0. \tag{31a}$$

To be perfectly consistent account should be taken of the fact that

$$\phi \to \eta - \Delta \quad \text{and} \quad \phi' \to 1 \quad \text{as} \quad \eta \to \infty,$$

where Δ is a constant related to the displacement thickness of the Hiemenz boundary layer. Neglecting Δ next to large η, one then obtains

$$\omega_1'' + \eta\omega_1' + (1 - k_i^2)\,\omega_1 = 0 \tag{31b}$$

as the appropriate asymptotic equation.

This last equation has been extensively studied, and Mangler (1943) discusses its two linearly independent solutions, ω_{1a} and ω_{1b} say. As the essential initial values and slopes for each of the solutions Mangler gives

$$\omega_{1a}(0) = 1, \quad \omega_{1a}'(0) = -\sqrt{2}\,\frac{\Gamma[\frac{1}{2}(k_1^2+1)]}{\Gamma(k_1^2/2)} < 0,$$

and

$$\omega_{1b}(0) = 0, \quad \omega_{1b}'(0) = 1.$$

The corresponding solutions to the equation (31*a*), which is equivalent to (31*b*) for sufficiently large η, were obtained on an analogue computer, and, for the same initial values, the initial slopes are only slightly different from those given above.

The behaviour of these solutions at large η is also given

$$\omega_{1a} \sim \frac{e^{-\frac{1}{2}\eta^2}}{\eta^{k_1^2}}\left[1 - \frac{k_1^2(k_1^2+1)}{2\eta^2} + \ldots\right], \tag{32}$$

$$\omega_{1b} \sim \eta^{k_1^2-1}\left[1 + \frac{(1-k_1^2)\,(2-k_1^2)}{2\eta^2} + \ldots\right]. \tag{33}$$

It is seen that the first solution approaches zero for all k_1 in the interval $0 \leqslant k < \infty$. Furthermore, it vanishes quite rapidly; analogue computer studies of this solution reveal that, for $k_1 = 0$, ω_{1a} is virtually zero for $\eta > 4$. As k_1 is increased, the approach to zero becomes more rapid.

On the other hand the second solution is a decreasing function at large η only if $k_1 < 1$, and even then it vanishes relatively slowly. The most rapid approach to zero occurs when $k_1 = 0$, and the solution behaves as η^{-1}. In the limiting case $k_1 = 1$ the 'tail' becomes infinitely long. When $k_1 > 1$, ω_{1b} increases monotonously without limit. The point is then that the asymptotic behaviour of the initial, solitary, vorticity component is essentially dominated by the second solution, ω_{1b}. Thus, if $k_1 > 1$, ω_1 will not be amplified but will steadily decay from its initial magnitude (which would be prescribed at some large value of η) as it is transported towards the boundary layer. If $k_1 < 1$, the vorticity will grow in intensity as it is swept in from large to small η values. This is the case of interest here. The case $k_1 = 1$, which was treated in the previous paper, is a special one and has been named *neutral*. The neutral-scale vorticity is convected towards the wall, far from the wall, with no net amplification or attenuation and this indicates a perfect balance between the stretching effect and viscous dissipation.

The dimensionless neutral wavelength or scale is $\lambda_0 = 2\pi$. It happens to be roughly 10 times the displacement thickness of the classical Hiemenz boundary layer. Thus $k_1 \lesseqgtr 1$ means $\lambda \gtreqless \lambda_0$. *It is only the vorticity of larger than neutral scale which can be amplified in the stagnation-point flow.* The smaller-than-neutral-scale vorticity, if present in the approaching flow with a low intensity as is stipulated here, will only grow weaker as it moves towards the boundary layer and arrive there as a truly insignificant perturbation.

4. A numerical example

The particular case $k_1 = \frac{2}{3}$, corresponding to $\lambda_1 = 1{\cdot}5\lambda_0$, has been solved on an electronic analogue computer. Solutions were achieved by iteration and, except for errors due to truncation of the iteration process and, of course, to the limited accuracy of the computer, they are exact solutions to the problem posed. In addition to the velocity boundary layer, the temperature boundary layers corresponding to Prandtl numbers 0·70, 7·0 and 100 were treated simultaneously. In this section, these computations will be described and the results presented.

The iteration process is begun by assuming that in certain equations the spectral-interaction functions are small enough to be neglected. The solutions so obtained then permit approximate solution for the first- and second-harmonic components of the added vorticity and velocity, and, with these, first approximations to the previously neglected interaction functions may be constructed. The free parameter A plays an essential role in these steps; but, for the range of A considered here, the second-harmonic quantities are at least an order of magnitude smaller than their first-harmonic counterparts. As a consequence, the rapid tailing off of the Fourier elements continues so that, for practical purposes, harmonics higher than the second may be ignored completely.

The results of the calculation are relative in that they expose the relative sensitivities of the momentum and thermal boundary layers to the same vorticity

input. Through the parameter A the initial amplitude of the imposed vorticity distribution is adjusted so that the change in the mean velocity boundary layer, characterized by the function ϕ, is small. In this context 'mean' signifies an average over the ζ- or z-co-ordinate. It will be seen that the concomitant changes in the three thermal boundary layers, characterized by T_0, are significantly larger.

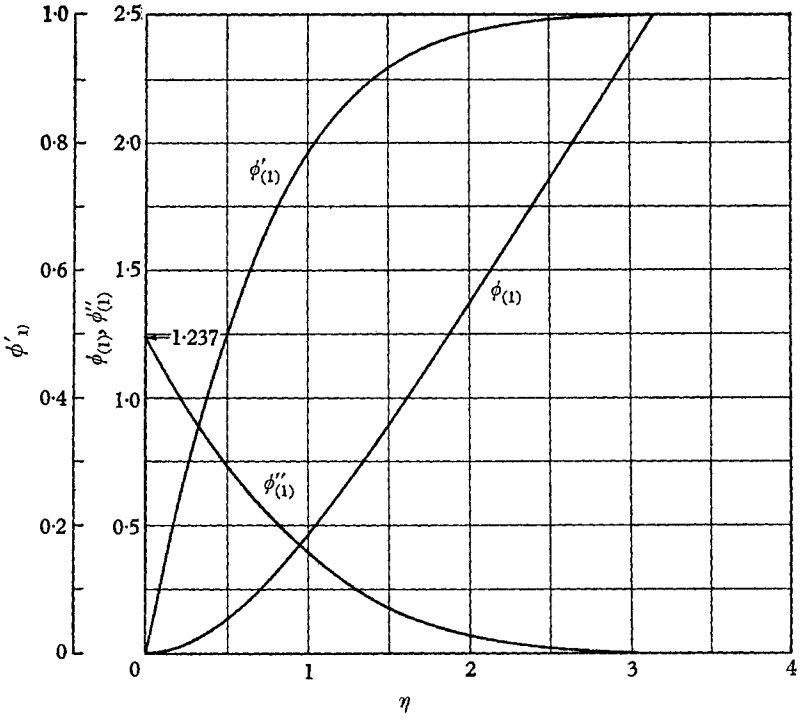

FIGURE 2. First approximation to the function ϕ, the Hiemenz solution.

The calculation begins with a first approximation to the function ϕ, denoted by $\phi_{(1)}$, obtained by solving the homogeneous version of equation (22)

$$\phi'''_{(1)} + \phi_{(1)}\phi''_{(1)} - \phi'^2_{(1)} + 1 = 0, \tag{34}$$

with the boundary conditions

$$\phi_{(1)}(0) = \phi'_{(1)}(0) = 0,$$
$$\phi'_{(1)} \to 1 \quad \text{as} \quad \eta \to \infty. \tag{35}$$

Such a solution describes the mean boundary layer when the distorting influence of the added vorticity is negligible, and the function $\phi_{(1)}$ is precisely the classical Hiemenz function. It is displayed in figure 2 as it was obtained from the computer. As a measure of the accuracy of the computation it is noteworthy that the function and its first two derivatives differ by less than 0·5 % from the best values obtained by Howarth (1935) and listed by Schlichting (1960).

With the function $\phi_{(1)}$, it is then possible to solve simultaneously for corre-

sponding first approximations to the mean temperature field T_0. Taken from the full equation (23), the approximate equation is

$$T''_{0(1)} + \Pr \phi_{(1)} T'_{0(1)} = 0, \tag{36}$$

subject to $$T_{0(1)}(0) = 0, \quad T_{0(1)} \to 1 \quad \text{as} \quad \eta \to \infty. \tag{37}$$

The solution to this system is precisely the temperature field for the Hiemenz flow when the wall and the far flow have constant temperatures. Solutions were obtained for three Prandtl numbers, and the temperature profiles are shown in figure 3. For purpose of comparison the function $\phi'_{(1)}$ characterizing the undistorted tangential velocity profile is also included.

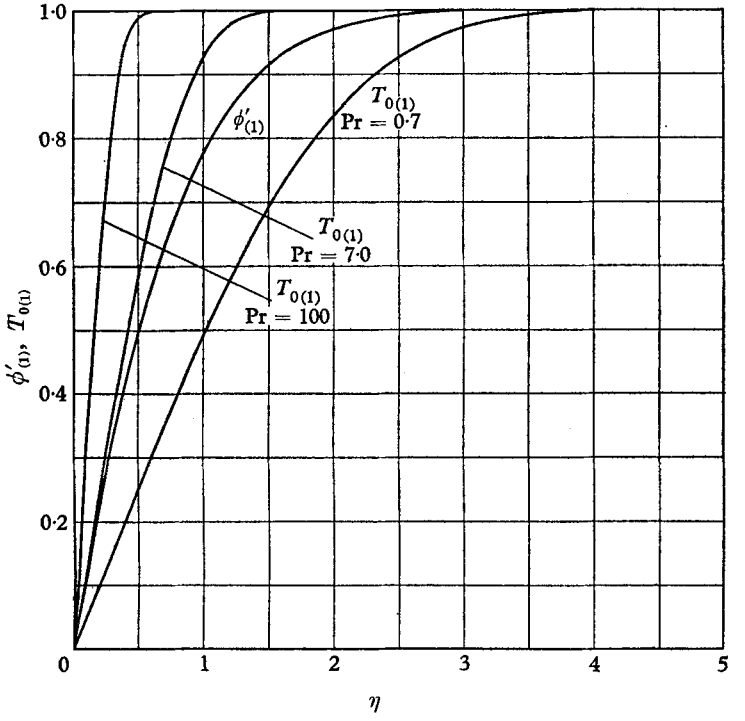

FIGURE 3. Temperature and velocity profiles before the addition of vorticity.

4.1. *First-harmonic components of vorticity and velocity*

Next, first approximations to the functions ω_1 and v_1 were obtained by simultaneous solution of the following approximate versions of equations (25) and (26)

$$-v''_{1(1)} + \tfrac{4}{9} v_{1(1)} = \tfrac{4}{3} \omega_{1(1)}, \tag{38}$$

$$\omega''_{1(1)} + (\phi_{(1)} \omega_{1(1)})' - \tfrac{4}{9} \omega_{1(1)} = 0, \tag{39}$$

with the boundary conditions

$$v_{1(1)} = v'_{1(1)} = 0 \quad \text{at} \quad \eta = 0,$$

and $$v'_{1(1)}, \quad v''_{1(1)}, \text{etc.} \to 0 \quad \text{as} \quad \eta \to \infty. \tag{40}$$

The second set of boundary conditions simply means that $v_{1(1)}$ must be a bounded function at large η. The approximate equations imply (i) negligible interaction

effects from higher harmonics and (ii) negligible coupling between the $v_1-\omega_1$ system and u_1. The latter supposition is not justified *a priori* and was actually forced on the calculation by shortage of computer capacity. Only after a first approximation for u_1 was in hand was it possible to assess the importance of the neglected coupling. The results below will verify that the coupling is indeed weak.

It is furthermore to be noted that $\omega_{1(1)}$, though apparently independent of $v_{1(1)}$, is actually coupled to the latter through the boundary conditions. There are no explicit boundary conditions on the vorticity but its initial value and slope must be chosen to satisfy the conditions of boundedness on $v_{1(1)}$. To see how this occurs one need only examine the general solution for $v_{1(1)}$. It is

$$v_{1(1)} = e^{-\frac{2}{3}\eta}\int_0^\eta e^{\frac{2}{3}\alpha}\omega_{1(1)}(\alpha)\,d\alpha - e^{\frac{2}{3}\eta}\int_0^\eta e^{-\frac{2}{3}\alpha}\omega_{1(1)}(\alpha)\,d\alpha.$$

If $v_{1(1)}$ is to be bounded, the integral multiplying the positive exponential must vanish at least as strongly as $e^{-\frac{2}{3}\eta}$. If the integral is to vanish at all, its integrand must change sign at least once. The factor $e^{-\frac{2}{3}\eta}$ does not change sign so $\omega_{1(1)}$ must. Now $\omega_{1(1)}$ is a linear combination of two independent functions (discussed in § 3)

$$\omega_{1(1)} = c_a\,\omega_{1a} + c_b\,\omega_{1b},$$

and neither of these functions changes sign in the interval $0 \leqslant \eta < \infty$. Thus the required behaviour for $\omega_{1(1)}$ can only be achieved by assigning values to c_a and c_b such that $\omega_{1(1)}$ changes sign and, when multiplied by $e^{-\frac{2}{3}\eta}$, gives an integral which vanishes sufficiently rapidly. For one thing, this would obviously require that $\omega_{1(1)}(0)$ and $\omega'_{1(1)}(0)$ have different signs.

Since equation (39) is linear and homogeneous there must be an arbitrary constant factor associated with its solution. This factor was adjusted so that the maximum magnitude of $v_{1(1)} = 1$ (on the machine scale). Hence the control of the absolute value of this maximum is left to the parameter A. Thus the physical significance that can be attached to A is that it represents the maximum magnitude attained by the amplitude of the imposed sinusoidal velocity variation, i.e. the $V_1(\eta)$ introduced at the beginning of § 2.2.

The solutions achieved for $v_{1(1)}$ and $\omega_{1(1)}$ are shown in figure 4. They indicate that between $\eta = 12$ and the edge of the classical boundary layer ($\eta \simeq 2{\cdot}4$) $v_{1(1)}$ is amplified by a factor of 10. The amplification ratio for $\omega_{1(1)}$ is about 15. Figure 5 shows how the ratio $r \equiv |v_{1(1)}|/|V_{0(1)}| = |v_{1(1)}|/\phi_{(1)}$ varies with η between $\eta = 12$ and the boundary. This ratio, which might be likened to a longitudinal turbulence intensity, undergoes a hundredfold amplification over the distance of five classical-boundary-layer widths. The fact that r exceeds unity means that locally the flow pattern may differ drastically from the Hiemenz flow which nevertheless continues to approximate the average flow pattern.

Also displayed in figure 4 are the functions $u_{1(1)}$ and $w_{1(1)}$. The former is obtained by solving an approximate version of equation (24)

$$u''_{1(1)} + \phi_{(1)}\,u'_{1(1)} - (2\phi'_{(1)} + \tfrac{4}{9})\,u_{1(1)} = \phi''_{(1)}\,v_{1(1)}, \tag{41}$$

subject to

$$u_{1(1)}(0) = 0, \quad \text{and} \quad u_{1(1)} \to 0 \quad \text{as} \quad \eta \to \infty. \tag{42}$$

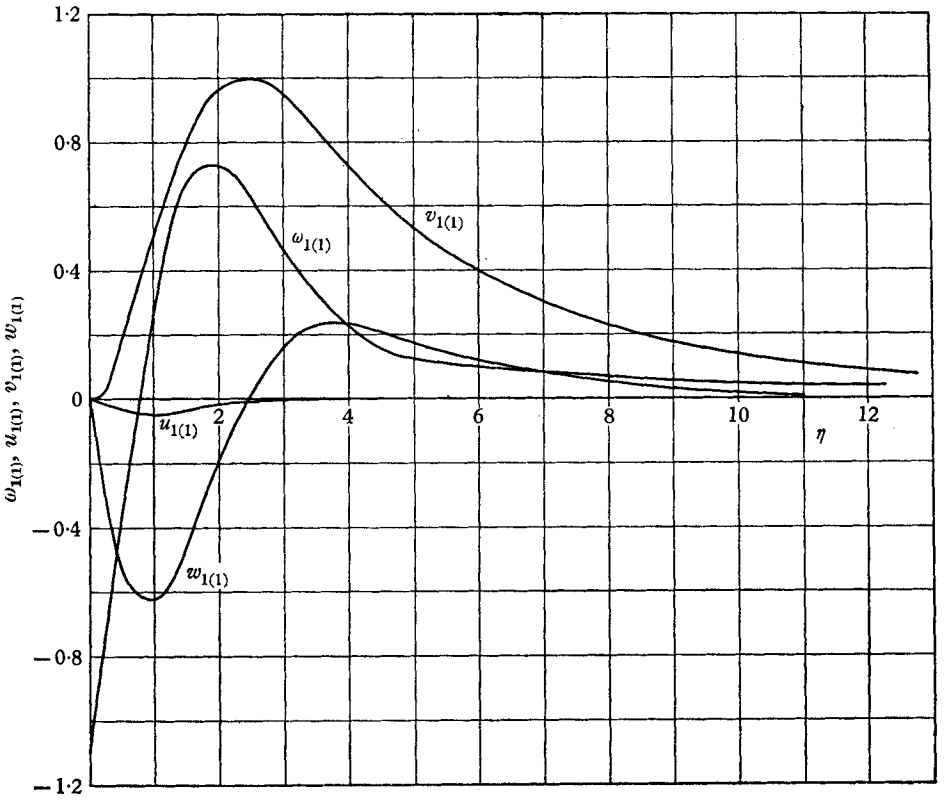

FIGURE 4. First approximations to the first-harmonic components of vorticity and velocity, $k_1 = \frac{2}{3}$.

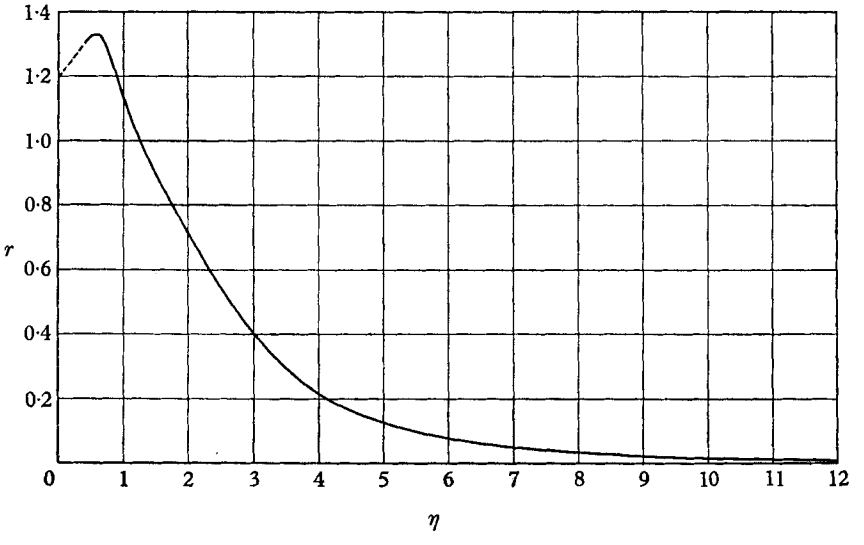

FIGURE 5. Relative intensity amplification of the first-harmonic component of normal velocity, $r = |v_{1(1)}|/|V_{0(1)}|$.

The function $\phi''_{(1)} v_{1(1)}$ was programmed on a variable function generator which simulates a function from ten straight line segments. The smallness of $u_{1(1)}$ compared to $v_{1(1)}$ and $\omega_{1(1)}$ is striking. The maximum value of $|u'_{1(1)}|$, which was neglected in equation (38), is 0·076, occurring at $\eta = 0$ where $|\omega_{1(1)}| \doteqdot 1{\cdot}1$. The estimated maximum error in the solutions for $v_{1(1)}$ and $\omega_{1(1)}$ due to the neglect of this term is about 5 %.

The function $w_{1(1)}$ is obtained by simple addition according to the algebraic relationship (19). Thus

$$w_{1(1)} = -v'_{1(1)} - u_{1(1)}.$$

It is interesting to note that the large variations in the normal velocity component v which exist near the boundary are almost entirely compensated by the induced axial component w. The tangential component u is hardly affected.

4.2. *Second-harmonic components of vorticity and velocity*

The second-harmonic components v_2 and ω_2 owe their existence, so to speak, to the interaction between the first-harmonic components and the main flow. Consequently some approximate representation of this interaction must be retained in the governing equations if any solution is to be achieved. Another, purely mathematical, reason for the necessity of this lies in the earlier discussion of the asymptotic behaviour of the homogeneous version of equation (26). This equation has two bounded solutions only when $k_n < 1$ and in the present case $k_2 = \frac{4}{3}$. The non-homogeneous equation, however, possesses a general solution which consists of these two complementary functions plus a particular integral. The latter effectively offsets the unbounded complementary function and makes possible a bounded solution for ω_2 which also satisfies the requirements on v_2.

The approximate equations and boundary conditions taken as governing $v_{2(1)}$ and $\omega_{2(1)}$ are

$$-v''_{2(1)} + \tfrac{16}{9} v_{2(1)} = \tfrac{8}{3} \omega_{2(1)}, \tag{43}$$

$$\omega''_{2(1)} + (\phi_{(1)} \omega_{2(1)})' - \tfrac{16}{9} \omega_{2(1)} = \tfrac{1}{2} A[(\omega_{1(1)} v_{1(1)})' + 2 w_{1(1)} \omega_{1(1)}], \tag{44}$$

$$\left.\begin{aligned} v_{2(1)} = v'_{2(1)} = 0 \quad &\text{at} \quad \eta = 0, \\ \text{and} \qquad v'_{2(1)}, \quad v''_{2(1)}, \text{ etc.}, \to 0 \quad &\text{as} \quad \eta \to \infty. \end{aligned}\right\} \tag{45}$$

Again the function generator was used to generate a reasonable facsimile of the right member of (44). In the computations the factor $\frac{1}{2}A$ was simply controlled by a potentiometer setting so that the output voltages simulating the variables $v_{2(1)}$ and $\omega_{2(1)}$ were large enough to ensure accurate functioning of the various machine elements. The obvious linear dependence of $v_{2(1)}$ and $\omega_{2(1)}$ on A then permits a simple scaling for any value of A whatsoever. The solutions for $v_{2(1)}$ and $\omega_{2(1)}$ corresponding to $A = 1$ are given in figure 6.

Also shown in figure 6 are the solutions for $u_{2(1)}$, obtained by solving

$$u''_{2(1)} + \phi_{(1)} u'_{2(1)} - (2\phi'_{(1)} + \tfrac{16}{9}) u_{2(1)} = \tfrac{1}{2} A[2\phi''_{(1)} v_{2(1)} + v_{1(1)} u'_{1(1)} - v'_{1(1)} u_{1(1)}], \tag{46}$$

$$u_{2(1)}(0) = 0, \quad u_{2(1)} \to 0 \quad \text{as} \quad \eta \to \infty, \tag{47}$$

and the function

$$w_{2(1)} = -v'_{2(1)} - u_{2(1)}. \tag{48}$$

The function $v_{2(1)}$ within the bracket in the right member of (46) is normalized, i.e. as shown in figure 6 for $A = 1$.

It was alluded to earlier and now it is clearly evident that the entire group of second-harmonic components of the velocity and vorticity amplitudes is substantially smaller, about one to two orders of magnitude, when $A = 1$, than the first harmonics.

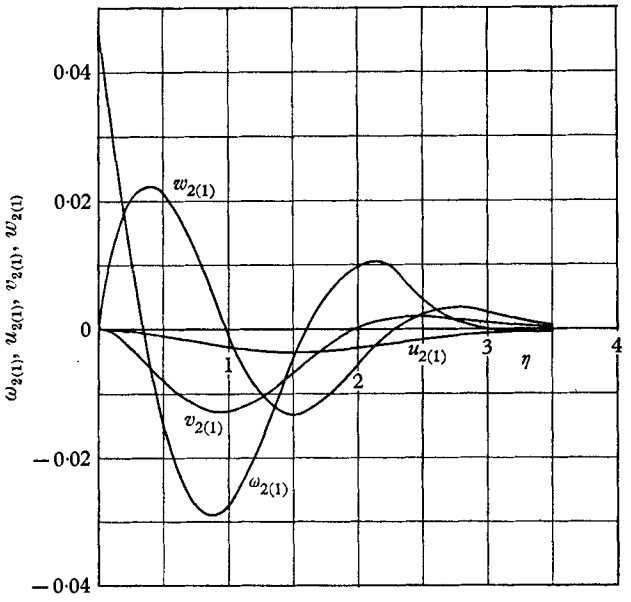

FIGURE 6. First approximations to the second-harmonic components of vorticity and velocity, $k_2 = \frac{4}{3}$. Magnitudes correspond to $A = 1$.

4.3. *Distortion of the mean velocity boundary layer*

A second approximation to the function ϕ, i.e. $\phi_{(2)}$, which shows, to first approximation, the distorting influence of the added vorticity on the mean flow, was obtained by solving

$$\phi'''_{(2)} + \phi_{(2)}\phi''_{(2)} - \phi'^2_{(2)} + 1 = A^2 M_{(1)}(\eta), \tag{49}$$

$$\phi_{(2)}(0) = \phi'_{(2)}(0) = 0, \quad \text{and} \quad \phi'_{(2)} \to 1 \quad \text{as} \quad \eta \to \infty, \tag{50}$$

where

$$M_{(1)} = u^2_{1(1)} + \tfrac{1}{2}(u_{1(1)} v_{1(1)})'. \tag{51}$$

It should be noted that, for the range of A considered below, the contribution of the second harmonics to the function $M_{(1)}$ amounted to less than 5 % of $M_{(1)}$ and so was not included. Figure 7 shows the function $\phi_{(2)}$ and its first two derivatives for several values of A. When $A = 0$, of course, $\phi_{(2)} = \phi_{(1)}$. The distortion is quite small for values of $A < 3$. In particular, when $A = 3$, the increase in the mean shear rate at the wall, i.e. $\phi''_{(2)}(0)$, is only 3·65 %. Also inserted in figure 7 is a plot of the function $M_{(1)}$ as it was generated by the variable function generator.

Figure 8 is a qualitative portrayal of the structure of the flow field near the boundary. No attempt has been made to duplicate the true relative scales in the profiles shown, but an idea is given of the periodic, cellular structure of the flow within the boundary layer. Obviously the particle paths are complex and it might be argued that the term 'boundary layer' has questionable significance in such a situation. The average flow pattern, however, is still characterized by a

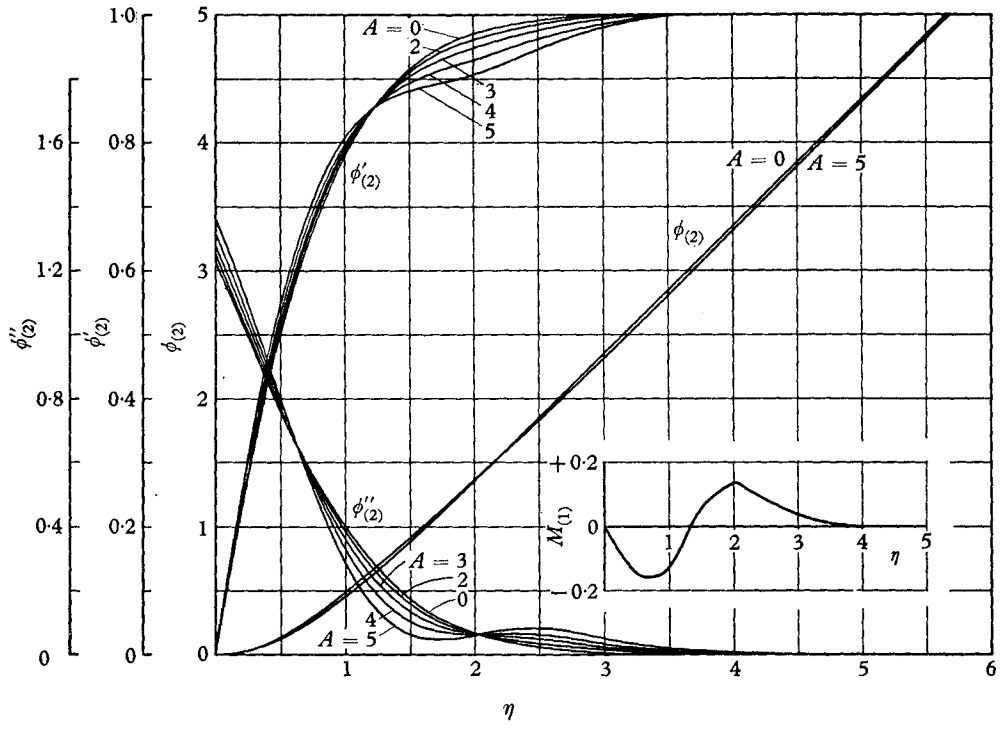

FIGURE 7. Approximate distortion of the mean flow field as a function of the amplitude parameter. $M_{(1)}$ represents approximately the distorting influence of added vorticity on the mean flow.

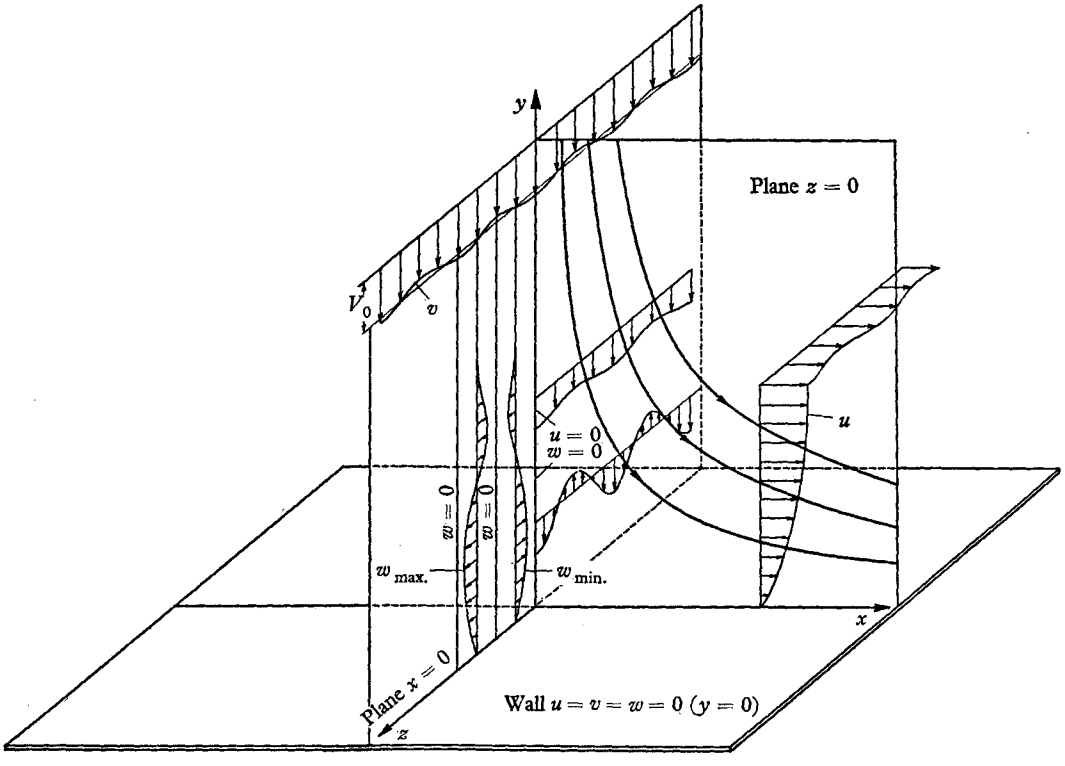

FIGURE 8. Qualitative representation of the flow pattern near the boundary.

definite boundary layer; and even locally the tangential-velocity profile, which differs little from the corresponding average profile $\phi'(\eta)$, defines a layer thickness which is practically constant for all values of z or ζ.

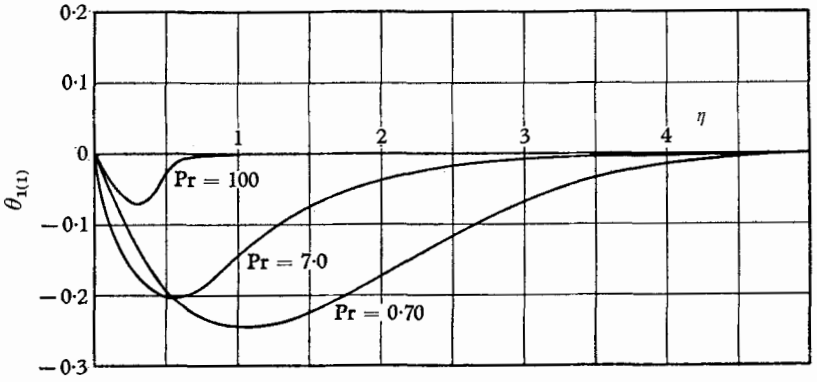

FIGURE 9. First approximations to the first harmonic components of the temperature function, $k_1 = \frac{2}{3}$.

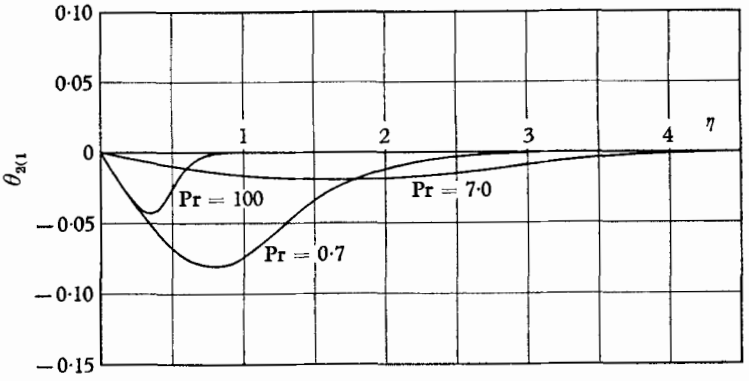

FIGURE 10. First approximations to the second harmonic components of the temperature function, $k_2 = \frac{4}{3}$. Magnitudes correspond to $A = 1$.

4.4. *Distortion of the mean temperature field*

The first- and second-harmonic components of the temperature distribution were calculated to first approximation from the following differential equations and boundary conditions:

$$\theta''_{1(1)} + \Pr \phi_{(1)} \theta'_{1(1)} - \tfrac{4}{9} \theta_{1(1)} = \Pr T'_{0(1)} v_{1(1)}, \tag{52}$$

$$\theta_{1(1)}(0) = 0, \quad \text{and} \quad \theta_{1(1)} \to 0 \quad \text{as} \quad \eta \to \infty, \tag{53}$$

$$\theta''_{2(1)} + \Pr \phi_{(1)} \theta'_{2(1)} - \tfrac{16}{9} \theta_{2(1)} = \tfrac{1}{2} A \Pr [2T'_{0(1)} v_{2(1)} + (v_{1(1)} \theta_{1(1)})' + u_{1(1)} \theta_{1(1)} + 2w_{1(1)} \theta_{1(1)}], \tag{54}$$

$$\theta_{2(1)}(0) = 0, \quad \text{and} \quad \theta_{2(1)} \to 0 \quad \text{as} \quad \eta \to \infty. \tag{55}$$

Here again, it is the normalized $v_{2(1)}$ (figure 6) which appears within the bracket of the right member of equation (54). The solutions $\theta_{1(1)}$ and $\theta_{2(1)}$ are depicted in figures 9 and 10 respectively for Pr = 0·7, 7·0, and 100.

At this point it remains only to calculate a second approximation to the function T_0, i.e. $T_{0(2)}$, which exposes to first approximation the distorting influence of the added vorticity on the mean temperature field. The pertinent differential equation and boundary conditions are

$$T''_{0(2)} + \Pr \phi_{(1)} T'_{0(2)} = A^2 N_{(1)}, \tag{56}$$

$$T_{0(2)}(0) = 0, \quad \text{and} \quad T_{0(2)} \to 1 \quad \text{as} \quad \eta \to \infty, \tag{57}$$

where

$$N_{(1)} \equiv \tfrac{1}{2} \Pr [u_{1(1)} \theta_{1(1)} + (v_{1(1)} \theta_{1(1)})']. \tag{58}$$

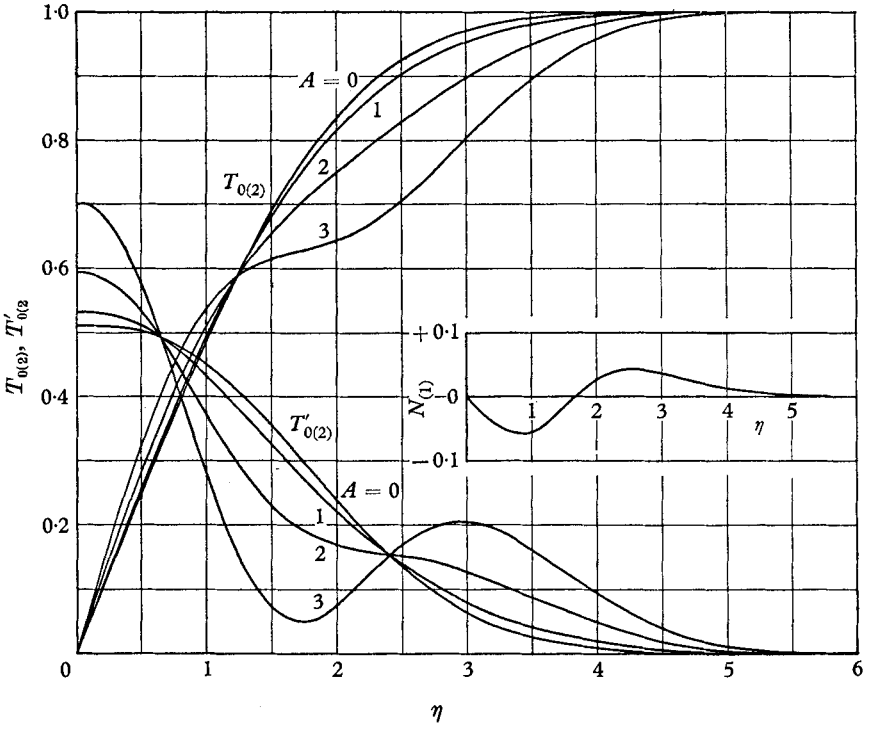

FIGURE 11. Distortion of the mean temperature field as a function of the amplitude parameter, Pr = 0·70. $N_{(1)}$ represents approximately the distorting influence of added vorticity on the mean temperature field.

Here, as in the case of $M_{(1)}$, the absence of second harmonics in the function $N_{(1)}$ indicates that, for the range of A considered, their contribution was negligible considering the overall computational precision maintained in the calculation. The functions $T_{0(2)}$ are shown for a few values of A in figures 11, 12 and 13 (in the case $A = 0$, $T_{0(2)} \equiv T_{0(1)}$). In all three cases the plots of $N_{(1)}$ as generated in the computer are inserted.

Table 1 summarizes the increments effected in the wall gradients of velocity (shear rate) and temperature (heat-transfer rate) for the four boundary layers treated. In each case, a quadratic dependence of the increments on A is discernible. This is to be expected in the behaviour of equation (56), which is linear, but it is interesting that it also holds for the non-linear equation (49). Comparison of the increments in the case $A = 2$ reveals that the temperature boundary layer

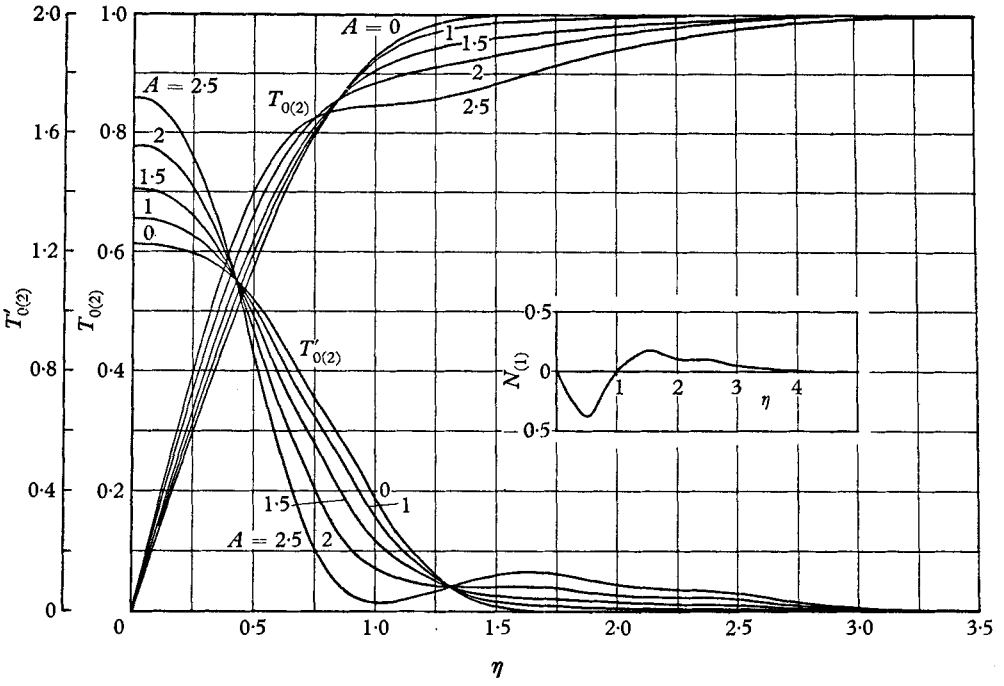

FIGURE 12. Distortion of the mean temperature field as a function of the amplitude parameter, Pr = 7·0.

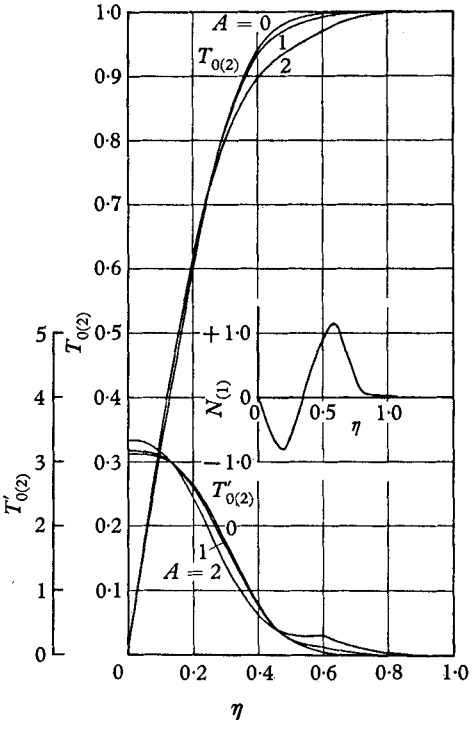

FIGURE 13. Distortion of the mean temperature field as a function of the amplitude parameter, Pr = 100.

for Pr = 0·7 is about 10 times more sensitive than the velocity boundary layer while the temperature boundary layers for Pr = 7·0 and 100 are nearly 16 times and four times more sensitive, respectively.

4.5. *Reasons for the difference in sensitivity*

The results presented in Table 1 clearly establish a significant difference between the sensitivity of the momentum boundary layer and that of thermal boundary layers of *comparable thickness*. Possible reasons for this difference were discussed in the previous paper by Sutera *et al.* It seems appropriate to summarize briefly these reasons here.

			Pr = 0·70		Pr = 7·0		Pr = 100	
A	$\phi''(0)$	$\Delta\phi''(0)$ (%)	$T_0'(0)$	$\Delta T_0'(0)$ (%)	$T_0'(0)$	$\Delta T_0'(0)$ (%)	$T_0'(0)$	$\Delta T_0'(0)$ (%)
0	1·237		0·510	—	1·225	—	3·122	—
0·5	—	—	0·516	+1·18	1·250	+2·04	3·144	+0·70
1·0	1·242	+0·40	0·532	+4·31	1·312	+7·1	3·185	+2·01
2·0	1·258	+1·70	0·595	+16·7	1·555	+26·9	3·350	+7·37
2·5	—	—	0·641	+25·7	1·716	+40·0	—	—
3·0	1·282	+3·65	0·703	+37·8	—	—	—	—

TABLE 1. Summary of increments effected in mean values of shear rate and temperature gradient

First, it may be noted that the function $M_{(1)}$, which controls the distortion provoked in the mean velocity field and displayed in figure 6, is truly a small quantity next to unity. It is small because $u_{1(1)}$ and $u'_{1(1)}$, which figure prominently in the formation of $M_{(1)}$, are both very small. The term unity in the basic Hiemenz equation stems from the pressure gradient in the original boundary-layer equations. If $A^2M_{(1)}$ is thought of as an additional η-dependent increment to this pressure gradient, then, for $A \simeq 1$, the increment is only 1 %. For $A = 3$, it is about 10 %, and perceptible changes begin to appear.

Examination of the functions $N_{(1)}$ shows that they are substantially larger than $M_{(1)}$; the smallest of the three, corresponding to Pr = 0·7, has maximum values more than twice those of $M_{(1)}$. The other two, it can definitely be said, are of order unity. These functions are larger than $M_{(1)}$ simply because the functions $\theta_{1(1)}$ and $\theta'_{1(1)}$ in the three cases are consistently and substantially greater than $u_{1(1)}$ and $u'_{1(1)}$ respectively. Since the principal contributors in the functions $M_{(1)}$ and $N_{(1)}$ are the terms $(u_{1(1)}v_{1(1)})'$ and $(\theta_{1(1)}v_{1(1)})'$, respectively, the influence of this circumstance is obvious.

Last, but not least, recognition must be given to the fact that, in one case, a third-order non-linear equation is being altered by the addition of a term, while, in the other case, it is a second-order linear equation, initially homogeneous. As far as the latter is concerned, it is perfectly correct to say that the change effected in the final solution is precisely the particular integral of the subsequently non-homogeneous equation. In the former case, no such clear-cut relationship between the solution and the added term exists. Another property of the non-linear equation believed relevant to a discussion of its sensitivity is the highly restrictive nature of the boundary conditions at the wall. The function $\phi_{(2)}$ and its

first derivative must both vanish at $\eta = 0$, and, in addition, the fact that $M_{(1)}(0) = 0$ effectively requires that $\phi'''_{(2)}(0) = -1$. Thus a distorting influence such as the added vorticity can affect the function $\phi_{(2)}$ near $\eta = 0$ only through its second, fourth and higher derivatives.

4.6. *Prandtl-number effect*

As previously reported the thermal boundary layer in a fluid with Pr = 7·0 is considerably more sensitive than that in the fluid with Pr = 0·7. This was corroborated by the present results. The calculation for the case Pr = 100 shows, however, that the sensitivity must attain a maximum for some Prandtl number and then diminish as Pr is increased further.

The explanation of this is simply that there are two mechanisms through which the Prandtl number affects the disturbed thermal boundary layer and these oppose one another. The first effect is to make the boundary layer thinner. This is brought about by the coefficient Pr in the left member of the differential equation (56). As this coefficient, and consequently the term it multiplies, become large, the curvature in the temperature profile can and does become correspondingly large locally. The result is a profile with rapidly decreasing slope and narrow in extent. The second, opposing effect is due to the coefficient Pr in the distorting function $N_{(1)}$. This coefficient magnifies the distorting influence and tends to provoke greater changes in the overall temperature profile. At some point, however, the profile becomes so narrow that the peaks of $N_{(1)}$ occur outside it, and the effectiveness of $N_{(1)}$ diminishes. That this should happen can be predicted by a simple physical argument. In the limit of infinite Prandtl number the energy transfer takes place in a zone next to the wall which is infinitesimally thin, and no distortions in the velocity profile short of violating the conditions of no slip and no through-flow can have any effect on it whatsoever.

4.7. *Comparison with the neutral-scale case*

The computations reported in the preceding paper were performed for added vorticity of neutral scale and a single value of the amplitude parameter, viz. $A = 8$. To summarize the effects obtained,

$$\Delta\phi''(0) = +4{\cdot}85\ \%,$$
$$\Delta T'_0(0) = +26{\cdot}0\ \% \quad \text{for} \quad \mathrm{Pr} = 0{\cdot}74,$$
and
$$\Delta T'_0(0) = +70{\cdot}0\ \% \quad \text{for} \quad \mathrm{Pr} = 7{\cdot}0.$$

In the present case a value of A slightly greater than three produces a comparable rise in the wall-shear rate, while $A = 2{\cdot}5$ gives a 26 % increase in the heat transfer rate for Pr = 0·70. It is estimated that a value of $A \doteq 3{\cdot}5$ would increase the heat transfer rate by 70 % for Pr = 7·0.

This all indicates that the larger-scale vorticity is more effective in producing distortions in the boundary layers, both dynamic and thermal, than is the neutral. A comparison of the solutions for the first harmonic components of the velocity and vorticity amplitudes in the two cases (neutral and 1·5 times neutral) indicates the reason for the difference. The larger-scale quantities, particularly v_1 and ω_1, undergo amplification and attain their peak values much closer to the

boundary, in fact within the mean boundary layer described by ϕ. In the neutral-scale case, v_1 and ω_1 approach the boundary layer with unvarying magnitudes and then decrease monotonously. The former begins its decline nearly two boundary-layer widths from the wall. As a consequence, the various cross products which make up the distorting functions are considerably reduced, and a much larger amplitude factor is needed to produce a change of a given magnitude.

5. Conclusions

A mathematical model introduced in an earlier paper (Sutera *et al.* 1963) has demonstrated the possibility of vorticity amplification by stretching in quasi two-dimensional stagnation flow. According to the model, amplification can occur if the vorticity scale is larger than a certain neutral scale, which is convected towards the boundary layer with no net amplification or attenuation. Smaller-scale vorticity only attenuates as it approaches the boundary layer.

Previously reported calculations revealed that the mean thermal boundary layer was much more sensitive than the mean momentum boundary layer to the presence of neutral-scale vorticity. In the present work the main flow transports vorticity of scale 1·5 times the neutral. This vorticity is amplified to a maximum value near the edge of the mean flow boundary layer and is generally more effective than the neutral scale in causing distortions in the flow and energy transport near the boundary. The substantially greater sensitivity of the thermal boundary layer is again demonstrated but it is shown that this sensitivity gradually decreases as the Prandtl number increases. Numerical results have been obtained for Prandtl numbers 0·70, 7·0 and 100. The increase in the heat-transfer rate at the boundary due to the addition of vorticity is greatest in the second case and least for the third case. The increases in heat-transfer rate at the boundary range from 4 to 16 times the concomitant increase in wall shear rate.

The work described in this paper constitutes part of a co-operative research programme on heat transfer in unsteady flows of the Aeronautical Research Laboratories, Office of Aerospace Research of the U.S. Air Force, under the technical supervision of Dr M. Scherberg. The financial support from this source as well as additional support from a National Science Foundation grant are gratefully acknowledged.

REFERENCES

HIEMENZ, K. 1911 Die Grenzschicht an einem in den gleichförmigen Flüssigkeitsstrom eingetauchten geraden Kreiszylinder. *Thesis, Göttingen and Dingl. Polytech. J.* **326**, 321.

HOWARTH, L. 1935 On the calculation of steady flow in the boundary layer near the surface of a cylinder in a stream. *Aero. Res. Counc., Lond., R&M* no. 1632.

KESTIN, J., MAEDER, P. F. & WANG, H. E. 1961 On boundary layers associated with oscillating streams. *Appl. Sci. Res.* A, **10**, 1.

KUETHE, A. M., WILLMARTH, W. W. & CROCKER, G. H. 1959 Stagnation point fluctuations on a body of revolution. *Phys. Fluids*, **2**, 714.

MANGLER, W. 1943 Die 'ähnlichen' Lösungen der Prandtlschen Grenzschichtgleichungen. *Z. angew. Math. Mech.* **23**, 241.

SCHLICHTING, H. 1960 *Boundary Layer Theory* (transl. J. Kestin). New York: McGraw-Hill.

SUTERA, S. P., MAEDER, P. F. & KESTIN, J. 1963 On the sensitivity of heat transfer in the stagnation-point boundary layer to free-stream vorticity. *J. Fluid Mech.* **16**, 497.